# Harmonic Mitigation in Inverter Circuits Through Innovative LC Filter Design Using PSIM

Habib Muhammad Usman[1,2], Muhammad Mahmud[1], Sani Saminu[3], Salihu Ibrahim[4]
[1]Department of Electrical Engineering, Ahmadu Bello University, Zaria, Nigeria
[2]Department of Electrical Engineering, Mewar University, Chittorgarh, Rajathan, India
[3]Department of Biomedical Engineering, University of Ilorin, Ilorin, Nigeria
[4]Department of Electrical Engineering, Waziru Umaru Federal Polytechnic, Birnin Kebbi, Nigeria

**ARTICLE INFO**

**Article history:**

Received February 11, 2024
Revised March 06, 2024
Published March 17, 2024

**Keywords:**

Harmonic Distortions,
HVDC Transmission,
LC Filter,
PSIM Software,
Three-Phase Inverter,
IGBT

**ABSTRACT**

The increasing use of renewable energy sources, such solar and wind power, and the growing ubiquity of High Voltage Direct Current (HVDC) transmission systems to improve power transmission efficiency are the main factors behind the increased deployment of inverter circuits. High harmonic distortions in the resultant sine wave, however, are a major problem for inverter circuits and could jeopardise circuit efficiency if left unchecked. This study presents a novel, affordable, and effective LC filter that is intended to remove almost all harmonic content from inverter circuits. The study uses PSIM software for the modelling, design, and control of a three-phase inverter. Starting with DC power supply, the study makes use of effective three-legged IGBT (insulated gate bipolar transistor) semiconductor devices as switch elements due to their high and current rating as well as faster operation. The switching gate pulses that turn inverter switches on and off at regular 60-degree intervals are produced by the pulse controller that controls the switches. This study's results show that the innovative LC filter in the inverter significantly reduced total harmonic distortion (THD) in all phases of the power signal. Specifically, THD decreased from 37.68% to 0.47% in the red phase, from 37.69% to 0.48% in the blue phase, and from 37.71% to 0.48% in the yellow phase. This reduction results in a notable improvement in power quality in all phases of the signal. Additionally, there is a noticeable increase in voltage magnitude, stabilizing and raising levels from 17.92 V to 23.83 V in the red phase, 17.93 V to 23.81 V in the blue phase, and 17.83 V to 23.81 V in the yellow phase due to the LC filter. These results demonstrated the effectiveness of the LC filter-equipped inverter for industrial, HVDC, and renewable energy applications.



**Corresponding Author**:

Habib Muhammad Usman, Department of Electrical Engineering, Ahmadu Bello University, Zaria, Nigeria & Department of Electrical Engineering, Mewar University, Chittorgarh, Rajathan, India
Email: habibusman015@gmail.com

## 1. INTRODUCTION

In the rapidly evolving landscape of power electronics, the pivotal role of inverter circuits has become increasingly pronounced, fueled by the escalating integration of renewable energy sources and advancements in High Voltage Direct Current (HVDC) transmission systems. As we usher in a new era of energy utilization, the demand for efficient, reliable, and clean power conversion technologies has never been more critical to our modern society [1]-[3]. But despite all of the advancements, one enduring problem remains: excessive harmonic aberrations in the sine wave output of inverter circuits. The overall effectiveness and dependability of power conversion systems are seriously threatened by these distortions if they are not corrected. In order to transform the traditional inverter circuit paradigm, this study explores this topic in great detail. In our modern culture, electricity is essential to many of our daily tasks. Because electricity is a necessary resource, having a steady and dependable supply is essential to making daily tasks easier. Electricity is produced using a variety of sources, including nuclear, solar, wind, hydro, fuel cells, and, more recently, gas [4], [5].

The inverter converts a direct current (DC) power source into an alternating current (AC) power source through a process called inversion. Contrary to this inversion process, rectification transforms an AC power source into a DC power source [6]-[8]. An inverter's principal purpose is to continuously supply AC power to connected loads, guaranteeing electricity even in the event that the main AC supply is unavailable. Its integration of a battery, charger circuit, and inverter circuit allows it to transform battery-stored DC power into AC power that can be used for devices like computers in the event of a mains power outage. The battery is kept charged for later use via the charger circuit. The majority of electronic devices run on DC power internally, while their exterior circuits require AC power [9], [10]. The inverter is less noisy, provides a complete automatic switchover function, poses no environmental threats, is less bulky, and is less expensive to maintain [11]. Fig. 1 shows the basic steps involved in inverter circuit.

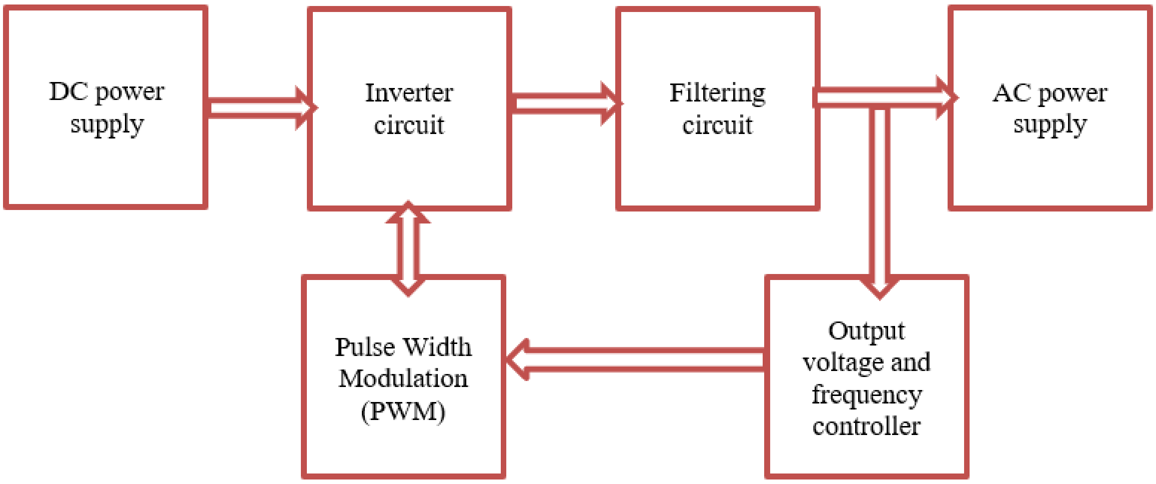

**Fig. 1.** Schematic diagram of an inverter

As shown in Fig. 1, inverter circuit starts with the DC input that come from a number of sources. It could originate from rectified AC mains in an industrial context, for example, or from a DC power supply that uses renewable energy sources, such as wind turbines or solar panels. Usually, the needs of the linked loads are taken into consideration while selecting the DC voltage level [12], [13]. Three pairs of power switches, one for each phase, make up the three-phase bridge arrangement. An IGBT (Insulated Gate Bipolar Transistor) and a diode make up each switch. This configuration makes it possible to convert DC power into three-phase AC power. The switches are controlled in such a way that the currents through them are modulated to create the desired sinusoidal output waveforms [14]-[17]. Pulse Width Modulation (PWM is a modulation technique that effectively and rapidly turns on and off power devices to manage the average voltage supplied to the load. Three-phase inverters regulate the output voltage of each phase by applying PWM to each leg of the bridge independently. The output frequency is determined by the PWM signal's frequency, and the output voltage amplitude is determined by the signal's duty cycle [18]-[22]. Output filtering in three-phase inverters is critical for ensuring that the output voltage waveforms are smooth and sinusoidal. This involves the use of filter such as LC (inductor-capacitor) or RC OR LCL or any suitable filters to remove high-frequency harmonics generated by the PWM switching. Additionally, balancing circuits may be employed to ensure that the three-phase output voltages are balanced, which is essential for the proper operation of three-phase loads [23]-[26].

IGBT (insulated gate bipolar transistor) Switching because of their quick switching times and minimal conduction losses, IGBTs are preferred for high-power applications. IGBTs in three-phase inverters turn on and off in response to PWM signals produced by the control circuitry. For the inverter to operate efficiently and to minimize losses, the IGBTs must be switched correctly [27]-[30]. A three-phase inverter's control circuitry continuously observes the output voltage and frequency and modifies the PWM signals to keep them at the appropriate values. This rule is essential to guarantee grid compatibility or to fulfil the demands of particular loads. It is possible to employ closed-loop control systems, in which the PWM signals are continuously adjusted based on sensor feedback [31]-[33].

Engineers and researchers working in the subject of power electronics utilize PSIM (Power Electronics Simulation) software, which provides a comprehensive platform for modelling, simulating, and evaluating intricate circuits and systems. With PSIM's extensive collection of pre-built components and user-friendly graphical user interface (GUI), users may easily and quickly create circuit schematics and simulate their behaviour. The software employs powerful simulation engines capable of accurately solving mathematical models describing circuit dynamics, allowing users to perform transient, steady-state, and frequency domain analyses to evaluate performance under various operating conditions [34], [35]. Support for control system design, which lets users simulate and apply different control techniques for power electronic converters, is one of PSIM's primary capabilities. Before implementing their control algorithms in practical applications, engineers can evaluate the stability, precision, and responsiveness of their algorithms by simulating control loops, feedback systems, and pulse-width modulation (PWM) approaches. Furthermore, PSIM enables users to optimize circuit parameters and do sensitivity analyses, enabling them to attain targeted performance metrics like power factor, harmonic distortion, and efficiency [36], [37].

Many works have reported their designed model of inverter circuit with various filtering techniques, among them are Segun, O. *et al.* [4] whose performed an analysis regarding irregular provision of electricity in Nigeria by distribution companies, there arises a necessity to establish an alternative electricity source to compensate for this unreliability. They proposed that, a supplementary power sources like generators and, more recently, semiconductor power devices such as the bipolar transistor, thyristor, and notably MOSFET and IGBT have to be employed for power generation, often in conjunction with a DC battery, yielding a few kilowatts of electric power. Moreover, Senthikumar *et al.* [38] considered certain energy sources that produce direct current (DC), whereas a significant portion of our equipment operates on alternating current (AC). Consequently, conversion devices become essential, cost-effective inverter was designed to address this challenge. LCL filter was proposed with passive damping resistors for reliability, robustness, stability and light weight by [39] and mathematical was also proposed to calculate the maximum current ripples. In an effort to mitigate harmonics series and parallel damping resistor in LCL passive filter which resulted to reduced total harmonic distortions (THDs) was proposed [40].

Mishra P. *et al.* [41] Investigated that squirrel cage induction motor (SQIM) fed by pulse width modulated voltage and current source inverter (VSI) brought additional losses in addition to motor losses, proposed here was an efficient sinusoidal LC filter for performance and efficiency improvement. Multifunction Grid-Interfaced inverter with LCL filter based was modelled, analysed and designed, furthermore, a contrast between the prior approach and the suggested OHRC system was provided [42]. In order to reduce switching losses, the inverter used a “Boost in Boost, Buck in Buck” arrangement, in which only one power stage runs at high frequency. The “Boost” and “Buck” modes' conduction power losses were decreased due to the design's achievement of a minimum voltage drop in the filtering inductor inside the power loop, the authors investigated line of grid-tied, DC/AC inverters that can handle a wide range of input DC voltages [43]. Bin G. *et al.* [44] Presented a method of improving the performance of Maximum Power Point Tracking (MPPT) by combining a reliable second-order sliding mode control (SOSMC) with a passive LC power decoupling circuit such that double-frequency pulsation on the dc-link is successfully eliminated by incorporating the passive LC decoupling method, which significantly increases MPPT accuracy [45]. Authors proposed digital counters used in place of an analog transformer to create a Sinusoidal Pulse Width Modulation (SPWM) system at a lower cost. Essential parts of the three-phase inverter's internal architecture include the low-pass filter, gate driver, SPWM module, Phase-Locked Loop (PLL), and snubber circuit. Achieving smooth synchronization between the inverter and the grid requires the incorporation of a well-matched PLL scheme. The investigation achieved cost-effective method to SPWM design, ensuring effective and synchronized operation with the grid, by substituting digital counters for the analog transformer. Implementation of the filter elements on an inverter's output, the EGS002 module generates a pulse width modulation (PWM) signal that was used to in inverter prototyping along with a low-pass filter, voltage regulator, MOSFET bridge, and DC voltage source [46], on the other hand, new class of fractional-order LLCL (FOLLCL) filters, which provide adaptable properties by varying the orders of one capacitor and three inductors in the filter construction was presented [47].

Software from Matlab/Simulink, PSIM, and PSPICE was used to compare, analyse, and simulate inverter circuits [48]. Meanwhile, Tawfikur R. [49] proposed a design model for the three-phase inverter's switching mode. In a similar vein [50] presented mathematical modelling and investigation of a reduced order induction motor drive system. This study [51] presented the design and control of a Grid-Connected three-phase, three-level NPC inverter for the purpose of building an integrated photovoltaic system.

PSIM stands out due to its specialized focus on power electronics and its intuitive user interface, which makes it easier for engineers to design and simulate complex power electronic circuits efficiently. Unlike general-purpose software like MATLAB, PSIM is tailored specifically for power electronics applications, offering a wide range of built-in components and modules dedicated to inverters, converters, and filters. Moreover, PSIM's simulation engine is optimized for power electronics simulations, ensuring high accuracy and fast simulation speeds compared to general-purpose circuit simulators like SPICE [34], [35]. This enables researchers to quickly iterate through different designs and analyse their performance effectively. Furthermore, PSIM offers comprehensive modelling and simulation support for intricate parts like LC filters and three-phase inverters. With its vast collection of power electronic models and components, researchers can quickly add cutting-edge features like the LC filter into their designs and properly replicate their performance.

The methodology employed in this investigation involves the utilization of PSIM software for modelling, LC filter design, and control of a three-phase inverter. Drawing power from a DC source and incorporating advanced three-legged Insulated Gate Bipolar Transistor (IGBT) semiconductor devices, our approach combines theoretical rigor with practical efficiency. The intricate swing of inverter switches, choreographed by a pulse controller at regular intervals, further distinguishes our methodology, ensuring adaptability for both star and delta connection loads through the deliberate selection of the 180-degree conduction mode.

This study presents a significant contribution to the field of power electronics by addressing the challenge of harmonic mitigation in inverter circuits. Unlike previous studies that have often faced trade-offs between effectiveness and cost-effectiveness, this research introduces a novel approach aimed at achieving the highest efficiency at the lowest cost. Through the design and implementation of a special LC filter using PSIM software, the study demonstrates impressive harmonic reduction in inverter circuits, thus enhancing overall efficiency. Additionally, the research stands out by focusing on the design and modelling of an effective, lightweight, and affordable inverter circuit, leveraging PSIM software for simulation and analysis. By incorporating the unique LC filter into the inverter design and demonstrating its effectiveness in harmonic reduction, this study contributes to advancements in mitigating harmonic distortions in power electronic systems, crucial for improving circuit efficiency and reliability. The research underscores the importance of simulation tools like PSIM in optimizing power electronic circuits, providing engineers and researchers with valuable insights into circuit behaviour, performance, and optimization, ultimately driving advancements in renewable energy integration and power transmission efficiency.

## 2. METHODS

The methodology used in this study involves,

- Three phase inverter was designed and simulated using PSIM software.
- Efficient LC filter was designed and simulated using PSIM software.
- Designed inverter was integrated with the designed LC filter.
- The results was recorded and analysed.

### 2.1. Design of Three Phase Inverter Systems

The three-phase inverter has been designed and simulated using PSIM software. As shown in Fig. 2, the first step in an inverter circuit involves the utilization of a DC (Direct Current) power source. This DC power source serves as the initial energy input that is to be converted into AC (Alternating Current) power. The DC source can originate from various places, depending on the application. For instance, in renewable energy systems such as solar or wind power, the DC source might be derived from solar panels or wind turbines, where sunlight or wind energy is converted into electrical energy through the process of photovoltaic conversion or mechanical energy conversion, respectively. In industrial settings or grid-tied systems, the DC source might be obtained from rectified AC mains or a battery bank. Regardless of its origin, the DC source provides the necessary electrical energy that serves as the foundation for the subsequent conversion process carried out by the inverter circuit.

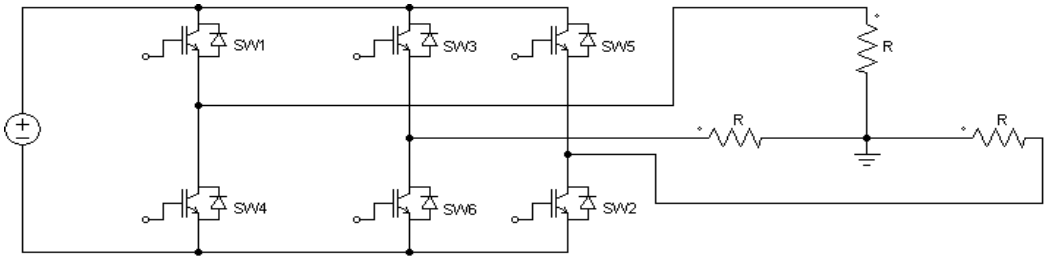


**Fig. 2.** The inverter switching logic circuit

$$V_{DC} = V_{source} - V_{drop} \tag{1}$$

where $V_{DC}$ = DC voltage input to the inverter, $V_{source}$= DC source voltage, $V_{drop}$= symbolizes any voltage drops that occur between the source and the inverter across components like wire, fuses, or diodes. The second step in inverter design involves the implementation of Pulse Width Modulation (PWM), a crucial technique used to regulate the average output voltage of the inverter by adjusting the width of pulses within a pulse train. In PWM, the duty cycle of the pulses, which represents the ratio of the ON time to the total period, determines the average voltage output. By varying the duty cycle, the effective voltage applied to the load can be precisely controlled. PWM is significant in inverter circuits as it allows for precise control of the output voltage, frequency, and waveform shape, ensuring compatibility with various loads and grid standards. Additionally, PWM helps in reducing harmonic distortions in the output waveform, thereby improving the overall quality of the AC power generated by the inverter. In this study, square wave PWM was employed due to several reasons. Firstly, square wave PWM is relatively simple to implement and computationally efficient, making it suitable for real-time control applications. Secondly, square wave PWM generates fewer harmonics compared to other PWM techniques such as sinusoidal or triangular waveforms, thus reducing the complexity of the filtering requirements. This simplifies the design and reduces the cost of associated components, making square wave PWM a practical choice for cost-effective implementations. Additionally, in this study, a PWM frequency of 5kHz was chosen. The choice of PWM frequency is crucial as it affects the efficiency, switching losses, and size of the filtering components. A higher PWM frequency allows for smoother waveform transitions, reducing audible noise and improving efficiency. However, excessively high frequencies can lead to increased switching losses and higher component costs. A PWM frequency of 5kHz strikes a balance between efficiency and cost-effectiveness, ensuring smooth operation while minimizing losses and component size.

$$D = \frac{T_{on}}{T_{on} + T_{off}} = \frac{T_{on}}{T_{period}} = T_{on} f_s \tag{2}$$

where $D$= Duty cycle, $T_{on}$= Time when the switch is ON, $T_{off}$= Time when the switch is OFF, $T_{period}$= Period and it is the sum of ON and OFF time, $f_s$ = Switching frequency which is the inverse of period.

The third step in inverter design involves the utilization of Insulated Gate Bipolar Transistors (IGBTs) as the switching devices within the inverter circuit. IGBTs are preferred over other switches such as MOSFETs or BJTs (Bipolar Junction Transistors) due to their advantageous combination of high current-carrying capability, fast switching speeds, and low conduction losses. These characteristics make IGBTs well-suited for high-power applications, such as inverter circuits, where efficient power conversion is essential. In an inverter circuit, IGBTs are responsible for rapidly switching the DC input voltage on and off according to the Pulse Width Modulation (PWM) control signals, thereby generating the desired AC output voltage. However, during the switching process, IGBTs incur switching losses, which contribute to energy dissipation and reduced efficiency of the inverter circuit. Switching losses primarily arise due to the finite switching times of the IGBTs and the inherent characteristics of the devices.

$$V_{CE} = V_{CE,sat} + V_{fwd} \tag{3}$$

where $V_{CE}$= Forward voltage drop across IGBT, $V_{CE,sat}$= Saturation voltage, $V_{fwd}$ = Forward drop due to conduction loss. The total power loss across IGBT is given in equation (4).

$$P_{total} = P_{cond} + P_{sw} \tag{4}$$

where $P_{total}$= total power loss across IGBT, $P_{cond}$= Power loss due to conduction of the switch and it depends on average collector current and saturation voltage, $P_{sw}$ = Switching loss which depends on switching frequency. These losses manifest as heat, which can adversely affect the performance and reliability of the inverter. To minimize switching losses, various techniques are employed. Firstly, optimizing the gate drive signals to reduce switching times can help mitigate losses. Additionally, implementing snubber circuits to dampen voltage spikes and ringing can reduce stress on the IGBTs and minimize losses. Furthermore, selecting IGBTs with lower conduction and switching losses can contribute to overall efficiency improvements. Moreover, advanced control strategies such as zero-voltage switching (ZVS) and zero-current switching (ZCS) can be utilized to further minimize switching losses, ultimately enhancing the efficiency and reliability of the inverter circuit. In the inverter design process, approximating the switching losses of IGBTs to zero is common due to their inherently fast switching speeds, low conduction losses, and meticulous optimization of gate drive signals and control strategies, which collectively contribute to minimal switching losses. Moreover, operating conditions are often tailored to minimize stress on the IGBTs, such as staying within safe temperature ranges and voltage/current limits, further reducing switching losses. Additionally, in practical applications, other losses in the system, such as conduction losses or losses in the filter components, may overshadow switching losses, especially at higher frequencies or specific load conditions. Therefore, by disregarding switching losses or approximating them to be negligible, it simplifies the analysis and design process without significantly compromising accuracy, allowing engineers to focus on optimizing more significant contributors to overall system efficiency and performance.

Finally, the inverter generates a three-phase AC output waveform, completing the conversion process from DC to AC power. This three-phase output is achieved by coordinating the switching of the IGBTs in a sequence that corresponds to the phases of the AC waveform. As mentioned earlier, the switches are triggered ON and OFF at regular intervals of 60 degrees, programmed to produce a balanced three-phase voltage. Each switch conducts for a duration of 180 degrees, ensuring a smooth transition between phases. By precisely controlling the timing and duration of the switch operations, the inverter generates a sinusoidal AC output waveform with three distinct phases, typically denoted as phase A, phase B, and phase C. This three-phase AC output is essential for powering three-phase loads and is commonly used in industrial and commercial applications where high-power electrical systems are required. The precise control provided by the inverter ensures that the generated AC waveform meets the required voltage, frequency, and waveform shape specifications, ensuring compatibility with various loads and grid standards.

The switches are triggered ON and OFF at regular intervals of 60 degrees as shown in Fig. 3. The sequence is programmed for a 3-phase voltage. There are two (2) possible patterns of control based on the length of the gating switches, which are the 120-degree mode in which switches remain ON for 120 degrees, and the 180-degree mode in which each switch conducts for 180 degrees. But the 180-degree mode was chosen in this project after simulating both patterns for its advantage that it can be used for both star and delta connection loads, unlike the 120-degree conduction mode that can be applied to only star connection loads.

The circuit operate in six (6) steps each step been 60 degree each switches is triggered after an interval of 60 degree and remain ON for 180 degree. Start with switch 1(SW1), which fired at 0 degree and conducted until 180 degree, while SW1 is conducting, SW2 fired when w=60 and remain ON to 240 degree, the pattern continued for SW3, SW4, SW5, SW6 and the sequence continued for another circuit of 360 degree as shown in Fig. 3.

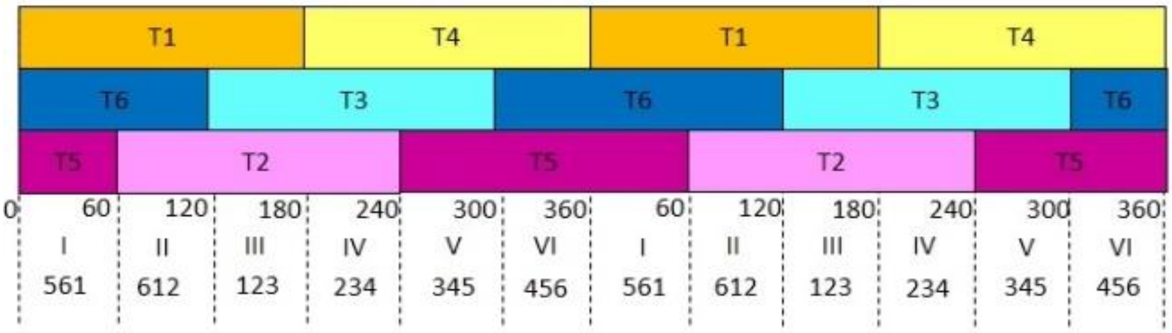


**Fig. 3.** The circuit pattern operation and the IGBT steps ON operations

For step 1 (0 to 60 degree) switches SW1, SW5 and SW6 are ON simultaneously, similarly. Step 2 switches SW6, SW1 and SW2 are ON. Step3 switches SW1, SW2 and SW3 are ON. Step 4 switches SW2, SW3 and SW4 are ON. Step 5 switches SW3, SW4 and SW5 are ON. Step 6 switches SW4, SW5 and SW6 are ON and the pattern repeated for further circuits.

### 2.2. Mode of operation

The mode of operation of an inverter circuit typically involves several steps to generate the desired AC output waveform. In a specific mode, such as mode 1 or mode 2 as described, the switches are triggered in a coordinated manner to achieve the desired voltage waveform.

#### 2.2.1. Mode 1

In mode 1, as shown in Fig. 4, the switches SW6, SW1, and SW2 are triggered simultaneously. This action results in the conduction of these switches, allowing the DC input voltage to flow through them and create a specific phase of the AC output waveform. By triggering these switches together, the inverter ensures that the output voltage follows the desired phase sequence, consistent with the intended three-phase

AC output. This coordinated switching action is important for generating a balanced and synchronized AC waveform across all three phases.

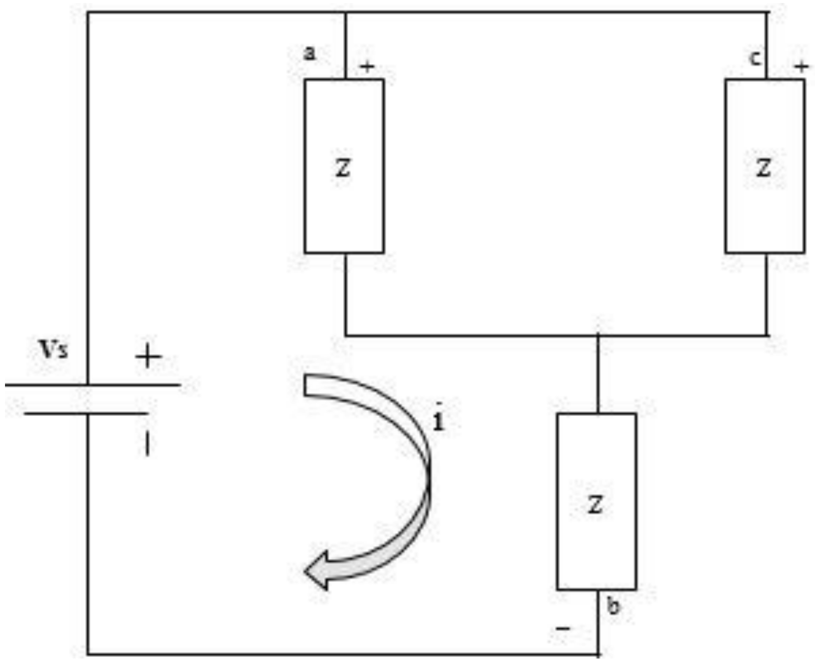


**Fig. 4.** Equivalent circuit of mode 1

### 2.2.2. Mode 2

Similarly, in mode 2, the switches SW5, SW3, and SW4 are simultaneously triggered. This coordinated activation of switches corresponds to a different phase of the AC output waveform, ensuring that the overall waveform remains balanced and synchronized across all three phases. By triggering specific switches simultaneously in each mode, the inverter circuit effectively creates the desired three-phase AC output, meeting the requirements of the load and ensuring compatibility with the grid or other connected systems. From ohm's law

$$V = IZ \tag{5}$$

$$I = \frac{V}{Z} \tag{6}$$

where: V is voltage source, I is the current, Z is the impedance. From Fig. 3.

$$i = \frac{Vs}{Z + \frac{Z}{2}} = \frac{2}{3}\frac{Vs}{Z} \tag{7}$$

where i is total current, $V_S$ the source voltage, $Z$ is the impedance. The total voltage across each resistor will be.

$$Vao = i.\frac{Z}{2} = \left[\frac{2}{3} . \frac{Vs}{Z}\right]\frac{Z}{2} = \frac{Vs}{3} \tag{8}$$

$$Vob = i.Z = \left[\frac{2}{3} . \frac{Vs}{Z}\right]Z = \frac{2}{3}Vs \tag{9}$$

$$Voc = i.Z = \left[\frac{2}{3} . \frac{Vs}{Z}\right]\frac{Z}{2} = \frac{Vs}{3} \tag{10}$$

where $V_{ao}$ line to neutral voltage drop across ao, $V_{oo}$ is line to neutral voltage drop across ob and $V_{oc}$ is line to neutral voltage drop across oc. And the same mode of operation and calculations apply to other steps (steps 2, 3, 4, 5, 6) and it will be seen that series load get more voltage drop and parallel load get lower voltage drop.

The three-phase line to neutral voltage to be plotted are $V_{ao}$, $V_{bo}$ and $V_{co}$. Using the values obtained from the calculation and the relationships above, Table 1 was formed. The values are plotted on the graph as shown in Fig. 5.

**Table 1.** Line to Neutral Voltages

| Step | $V_{ao}$ | $V_{bo}$ | $V_{co}$ |
|---|---|---|---|
| 1 | $\frac{1}{3}V_S$ | $\frac{-2}{3}V_S$ | $\frac{1}{3}V_S$ |
| 2 | $\frac{2}{3}V_S$ | $\frac{-1}{3}V_S$ | $\frac{-1}{3}V_S$ |
| 3 | $\frac{1}{3}V_S$ | $\frac{1}{3}V_S$ | $\frac{-2}{3}V_S$ |
| 4 | $\frac{-1}{3}V_S$ | $\frac{2}{3}V_S$ | $\frac{-1}{3}V_S$ |
| 5 | $\frac{-2}{3}V_S$ | $\frac{1}{3}V_S$ | $\frac{1}{3}V_S$ |
| 6 | $\frac{-1}{3}V_S$ | $\frac{-1}{3}V_S$ | $\frac{2}{3}V_S$ |

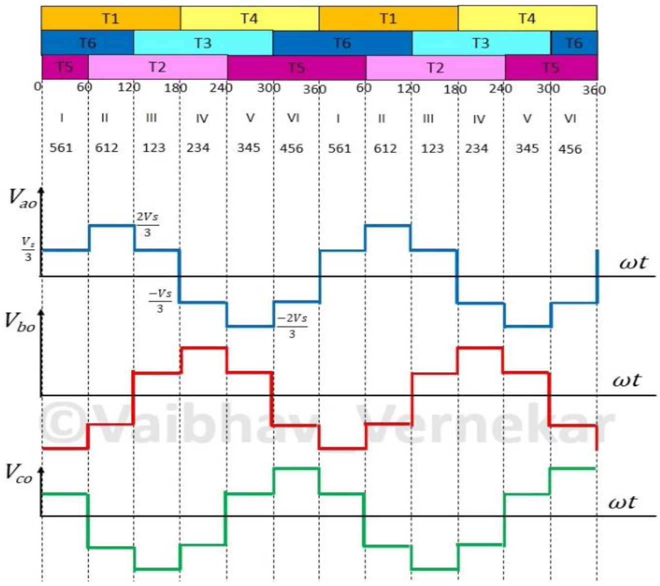


**Fig. 5.** Line to neutral plotted graph

### 2.3. Design of the Three Phase Inverter Systems on P-SIM

The three-phase inverter has been designed and simulated using PSIM software. The design is shown in Fig. 6. The input DC voltage used in this simulation was 24V, switching frequency of 5KHz, duty cycle of 50%,

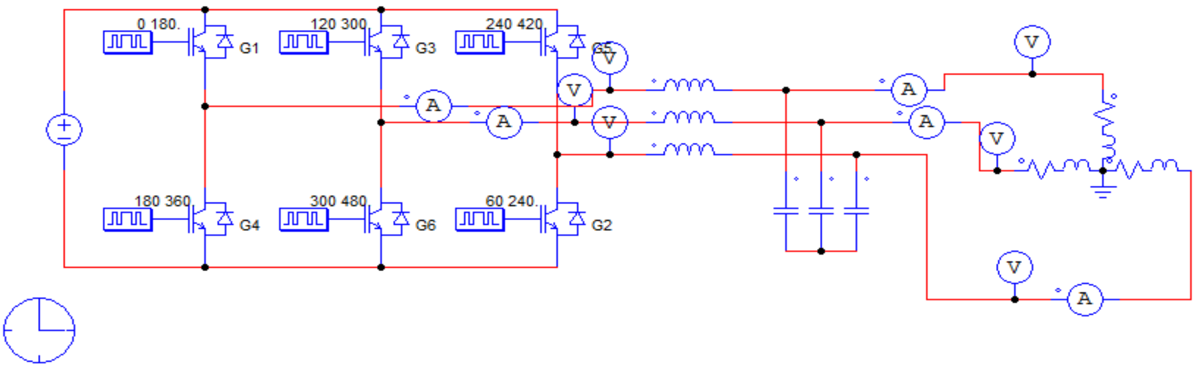


**Fig. 6.** The inverter switching logic circuit on PSIM

### 2.4. LC Filter Design on PSIM

Fig. 7 shows the LC output filter circuits design, which consist of an inductor and a capacitor. The LC low-pass filter is able to attenuate most low-order harmonics in the output voltage waveform. The switching frequency in high-power applications is chosen with regard to inverter efficiency since switching losses are a significant portion of the overall losses. It is desirable to minimize the size and cost of the filtering components by increasing the switching frequency (5 kHz was choosing in this paper). Because of its exact frequency selectivity, compact size, dependability, simplicity, low power losses, high efficiency, and high power handling capabilities, an LC filter is best suited for inverter circuits. With their simple, passive design, LC filters ensure good power transfer, efficient filtering of undesired harmonics and noise from the output waveform, and minimal cost and complexity. These inverters are perfect for a wide range of inverter applications, such as industrial motor drives, renewable energy systems, uninterruptible power supply, and electric vehicle powertrains. They can manage high power levels and offer exact frequency selectivity. Furthermore, the extended service life and dependability of passive parts like inductors and capacitors employed in LC filters add to the overall robustness and dependability of the inverter circuit.

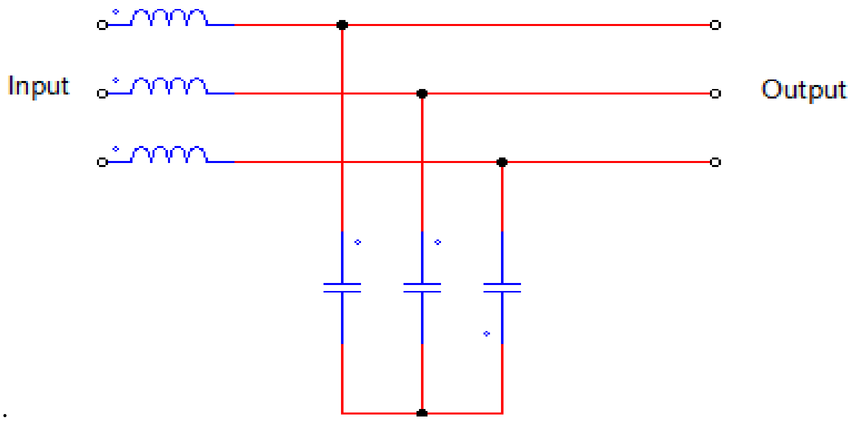


**Fig. 7.** LC filter circuit

Choosing a large inductor will require a similar capacitor in order to counterbalance the substantial voltage drops caused by load transients [24]. Impedance of the inductor and capacitor.

$$Z_L = j\omega L \tag{11}$$

$$Z_C = \frac{1}{j\omega C} \tag{12}$$

where $Z_L$ = Impedance of the inductor, $Z_c$ = Impedance of the capacitor, L = Inductance of the inductor, C = Capacitance of the capacitor, $\omega$= Angular frequency (2pi times frequency in Herz), j = imaginary unit. To find the cut-off frequency $f_c$ of the filter, where the filter starts to attenuate the higher frequency, this occurs when the reactance of inductor and capacitor are equal in magnitude but opposite in sign. Equating equation (7) and (8).

$$Z_L = Z_C = j\omega_C L = \frac{-1}{j\omega_C C} \tag{13}$$

$$\omega_C = 2\pi f_c \tag{14}$$

where $f_c$ = Cut-off frequency in Herz, substituting equation (14) in (13) and solving the equations yield.

$$f_c = \frac{1}{2\pi\sqrt{LC}} \tag{15}$$

This cut-off frequency is also referred to as switching frequency $f_s$. Inductor equation:

$$L = \frac{V_{DC}}{8 f_s \Delta I_O} \tag{16}$$

From equation (12), $V_{DC}$ = Voltage DC source = 24V. $f_s$ = Switching Frequency, The choice of switching frequency is crucial as it affects the efficiency, switching losses, and size of the filtering components. A higher switching frequency allows for smoother waveform transitions, reducing audible noise and improving efficiency. However, excessively high frequencies can lead to increased switching losses and higher component costs. Switching frequency of 5kHz strikes a balance between efficiency and cost-effectiveness, ensuring smooth operation while minimizing losses and component size. ΔIo = Maximum Current Ripple = 10% of the inductor current = 10% *5A = 0.5A.

$$L = \frac{V_{DC}}{8 f_s \Delta I_O} = \frac{24}{8 \times 5000 \times 0.5} = 1.2mH$$

By substituting the value of L in equation (15), we get the value of capacitor,

$$f_c = \frac{1}{2\pi\sqrt{LC}} = 5 \times 10^3 = \frac{1}{2\pi\sqrt{(1.2 \times 10^{-3} \times C)}}$$

$$C = 0.85 \times 10^{-6} Farad = 0.85\mu F$$

## 3. RESULTS AND DISCUSSION

The simulation results conducted using PSIM software were visually presented graphically. Both the inverter circuit with and without the filter were designed, and the total harmonic distortion (THD) was analysed alongside the measurement of voltage output levels. Furthermore, a comparison was drawn between the obtained results and experimental data to ensure validation. Subsequently, the findings were thoroughly discussed.

### 3.1. PSIM Simulation Results

The DC-source waveform, which is from a battery of 24 volts, as depicted in Fig. 8, was used as an input voltage source. In the design, a pulse width modulation with a duty cycle of 50% has been used to generate the sinusoidal wave, and a sampled phase signal has been used to synchronize the inverter output phase with the phase.

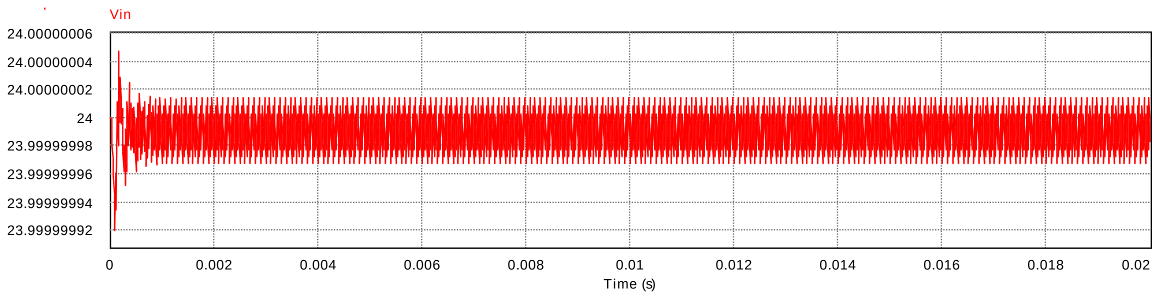


**Fig. 8.** Input controlled DC voltage source to the inverter circuit

Fig. 9 shows how harmonic content causes a considerable distortion in the red phase inverter's output voltage. Adding an effective filtering circuit is essential for improved performance in order to address this. The goal of this study is to minimize distortions and maximize system performance by developing an efficient and cost-effective LC filter that was simulated using PSIM software. Fig. 10 presents the almost perfect sine wave generated by the LC filter for the red phase voltage, thereby eliminating parasitic harmonic aberrations. To maximize the filter's efficiency, carefully measure the capacitor and inductor sizes and choose a 5 kHz switching frequency that strikes a balance between size, cost, and performance. Huge improvements in power quality are shown in Table 2, by comparing the line to neutral red phase voltage with and without an inventive LC filter. With the novel LC filter, the total harmonic distortion (THD) drops significantly from 37.68% without the filter to 0.47%, demonstrating a noteworthy reduction in harmonic distortion. Furthermore, the voltage magnitude rises from 17.92 V without the filter to 23.83 V with the filter, indicating that distortions or fluctuations in the voltage have been effectively mitigated, leading to a higher and more stable voltage level. The current magnitude, on the other hand, shows no change in current magnitude between the two cases, increasing slightly from 4.84 A without the filter to 4.98 A with the LC filter.

The output of the inverter, as shown in Fig. 11, exhibits a considerable distortion that can be attributed to harmonic content. This distortion has an undesirable effect on the efficiency of the inverter as well as the associated system. Fig. 12 shows an exceptionally clean sine wave with little distortion in the blue phase voltage. Table 3, shown Notable improvements in power quality are shown by comparing the line to neutral blue phase voltage with and without an innovative LC filter. With the novel LC filter, the overall harmonic distortion (THD) dramatically decreases from 37.69% without the filter to 0.48% with the filter, indicating a considerable reduction in harmonic distortion. Additionally, the voltage magnitude increases with the LC filter from 17.93 V to 23.81 V, suggesting that distortions or variations in the voltage have been effectively mitigated, leading to a higher and more stable voltage level. Meanwhile, the current magnitude shows negligible impact on current magnitude, maintaining relative consistency across the two scenarios with a tiny increase from 4.86 A without the filter to 4.97 A with the LC filter.

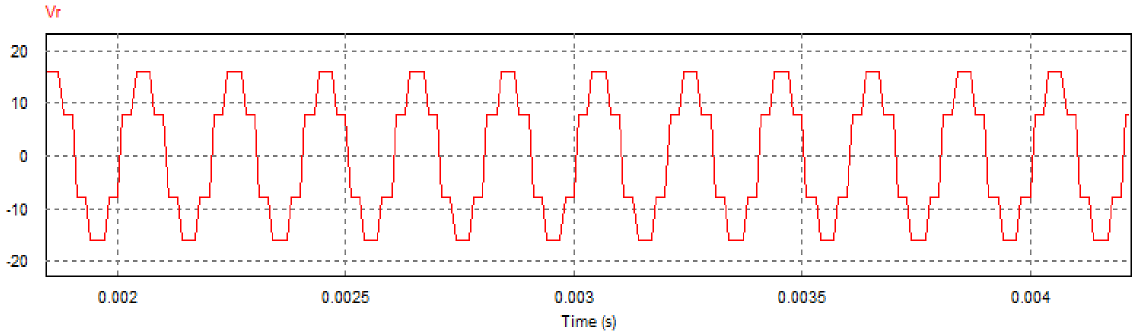


**Fig. 9.** Red phase output voltage of the inverter without filter

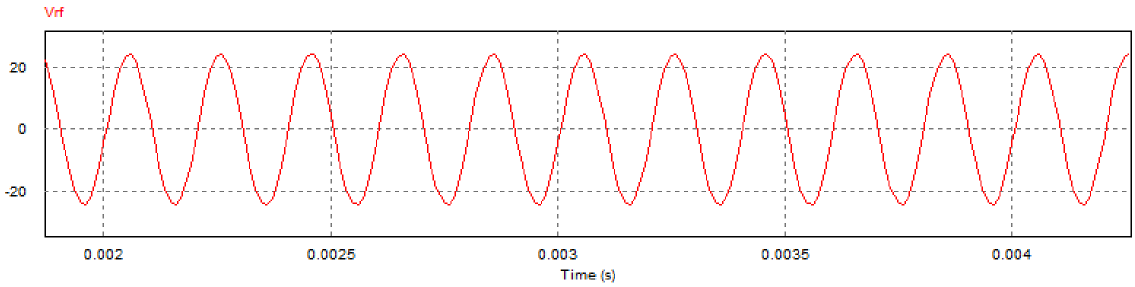


**Fig. 10.** Red phase output voltage of the inverter with innovative LC filter

**Table 2**: Red phase THD, voltage and current analysis

| | THD (%) | Voltage magnitude (V) | Current magnitude (A) |
|---|---|---|---|
| Without filter | 37.68 | 17.92 | 4.84 |
| With innovative LC filter | 0.47 | 23.83 | 4.98 |

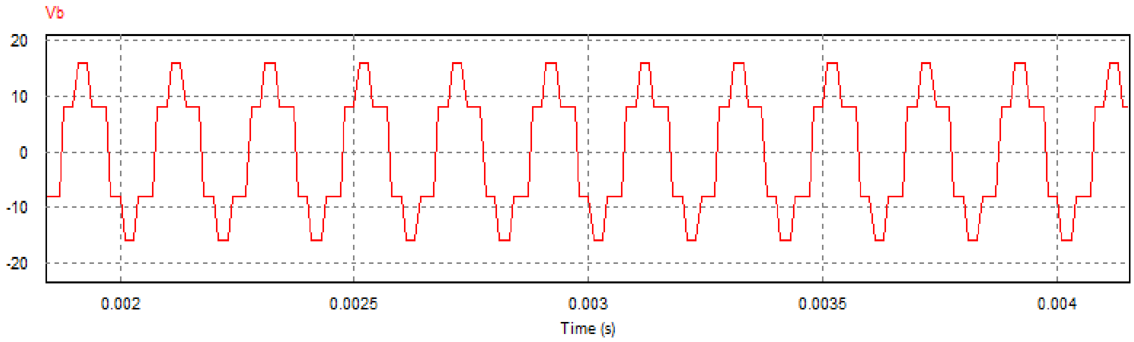


**Fig. 11.** Blue phase output voltage of the inverter without filter

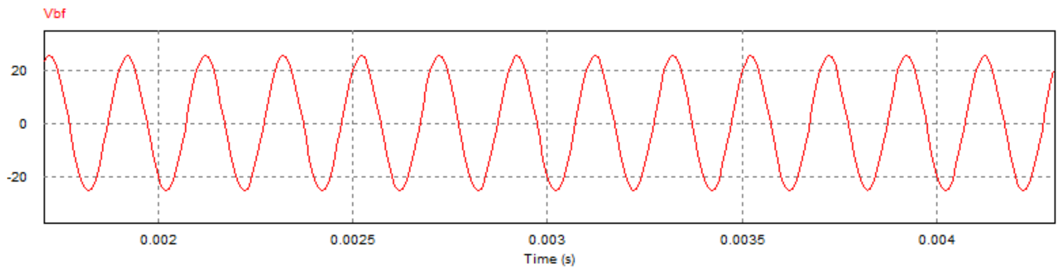


**Fig. 12.** Blue phase output voltage of the inverter with innovative LC filter

**Table 3.** Blue phase THD, voltage and current analysis

| | THD (%) | Voltage magnitude (V) | Current magnitude (A) |
|---|---|---|---|
| Without filter | 37.69 | 17.93 | 4.86 |
| With innovative LC filter | 0.48 | 23.81 | 4.97 |

Significant distortion is shown in the inverter output voltage for the yellow phase (Fig. 13), which has a negative effect on system efficiency. To address this, an effective and cost-effective LC filter is presented and simulated using PSIM software. When this filter is integrated, the yellow phase voltage produces a distortion-free sine wave (Fig. 14), demonstrating how well it reduces harmonic distortions. In high-power applications, optimizing the sizes of capacitors and inductors as well as selecting a switching frequency of 5 kHz improves the efficiency of the inverter. As shown in Table 4, Power quality has significantly improved when comparing the line to neutral yellow phase voltage with and without a novel LC filter. With the novel LC filter, the total harmonic distortion (THD) drops significantly from 37.71% without the filter to 0.48%, demonstrating a noteworthy reduction in harmonic distortion. Furthermore, the voltage magnitude increases with the LC filter from 17.83 V to 23.81 V, indicating that distortions or fluctuations in the voltage have been mitigated and that the voltage level has become greater and more stable. The current magnitude, on the other hand, shows little change in current magnitude between the two scenarios, increasing slightly from 4.86 A without the filter to 4.98 A with the LC filter.

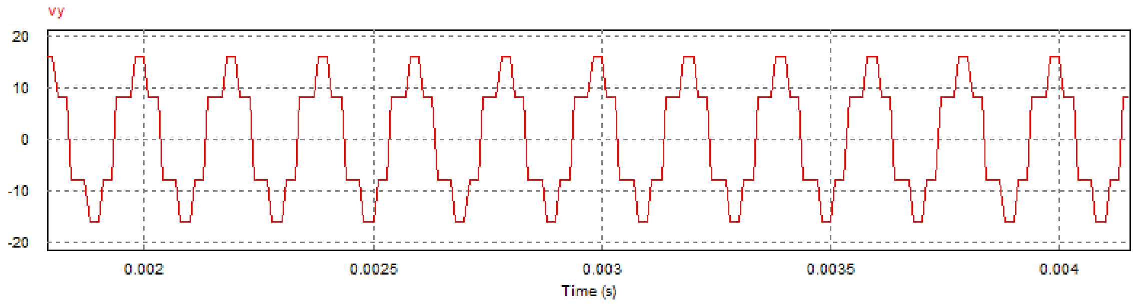


**Fig. 13.** Yellow phase output voltage of the inverter without filter

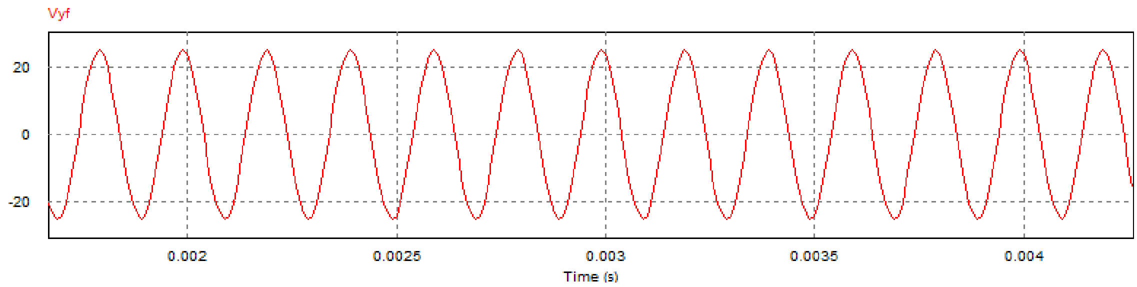


**Fig. 14.** Yellow phase output voltage of the inverter with innovative LC filter

**Table 4**. Yellow phase THD, voltage and current analysis

| | THD (%) | Voltage magnitude (V) | Current magnitude (A) |
|---|---|---|---|
| Without filter | 37.71 | 17.83 | 4.82 |
| With innovative LC filter | 0.48 | 23.81 | 4.95 |

### 3.2. Experimental validation

In a study conducted by Karami *et al.* [52] an experimental investigation was performed to evaluate the performance of a single-phase grid-connected inverter equipped with an LC filter for photovoltaic (PV) applications. The inverter was tested under various operating conditions, including different load levels and solar irradiance levels. The experimental results demonstrated a significant reduction in total harmonic distortion (THD) of the output voltage waveform with the implementation of the LC filter. Specifically, THD was reduced from 23.5% without the filter to 2.1% with the LC filter under full-load conditions. Additionally, the voltage waveform was found to be smoother and closer to a sinusoidal shape with the LC filter, indicating improved power quality.

In a study conducted by Li *et al.* [53] an experimental investigation was conducted to evaluate the performance of a three-phase grid-connected inverter with an LC filter for renewable energy applications. The inverter system was tested under varying load conditions and grid disturbances. The experimental results showed a significant reduction in total harmonic distortion (THD) of the output voltage waveform with the implementation of the LC filter. Specifically, THD was reduced from 8.6% without the filter to 1.2% with the LC filter under full-load conditions. Additionally, the voltage waveform exhibited reduced distortion and improved sinusoidal shape with the LC filter, indicating enhanced power quality. B. Rajesh *et al.* [54] utilized Matlab software in designing inverter circuit with and without filter and the result of his study was summarised in Table 5.

**Table 5**. Total harmonic distortion, voltage and current [54]

| | THD in % | Voltage (V) | Current (A) |
|---|---|---|---|
| Without filter | 32.44 | 63.1 | 3.59 |
| With filter | 1.4 | 64.88 | 3.69 |

The experimental results from references [52] and [53], as well as the simulation results from reference [54], provide valuable validation for the findings of this study regarding the effectiveness of the LC filter in mitigating harmonic distortion in inverter circuit. These studies utilized LC filters and demonstrated a significant reduction in harmonic distortion, with values ranging from 1% to 2.1%. Similarly, in this work, the implementation of the innovative LC filter resulted in a drastic reduction of harmonic distortion to 0.47% in the line to neutral red phase voltage and 0.48% in both the line to neutral blue and line to yellow phase voltages. This consistency in results across different studies reinforces the effectiveness of the innovative LC filter in mitigating harmonic distortion. The substantial reduction in harmonic distortion observed in your study compared to previous works further validates the efficacy of the innovative LC filter design. Therefore, the collective evidence from these studies provides strong support for the effectiveness of the innovative LC filter in enhancing power quality by reducing harmonic

### 3.3. Result discussion

The results of the study demonstrate a significant improvement in power quality when comparing the line to neutral red, blue, and yellow phase voltages with and without the novel LC filter. The implementation of the novel LC filter resulted in a remarkable reduction in total harmonic distortion (THD), dropping from 37.68% without the filter to 0.47% with the filter in the red phase, 37.69% to 0.48% in the blue phase, and 37.71% to 0.48% in the yellow phase. This substantial reduction in harmonic distortion emphasizes the effectiveness of the novel LC filter in improving power quality by minimizing harmonic content in the output voltage waveform. Moreover, the voltage magnitude experienced a notable increase with the LC filter, rising from 17.92 V to 23.83 V in the red phase, 17.93 V to 23.81 V in the blue phase, and 17.83 V to 23.81 V in the yellow phase. This increase in voltage magnitude suggests that distortions or fluctuations in voltage have been mitigated, resulting in a more stable and higher voltage level. Conversely, the current magnitude exhibited little change between the two scenarios without the filter and with the LC filter. This indicates that the innovative LC filter effectively mitigates voltage distortions without significantly impacting current levels. Again, these findings highlight the efficiency of the inverter equipped with the novel LC filter, making it suitable for industrial applications, high voltage direct current (HVDC) systems, and integration into renewable energy sources such as solar and wind.

## 4. CONCLUSIONS

In summary, this study presents a novel LC filter solution that effectively mitigates high harmonic distortions in inverter circuits, offering significant improvements in power quality across all phases of the signal. The findings demonstrate the practical viability of this approach in industrial, HVDC, and renewable energy applications, as evidenced by the substantial reduction in total harmonic distortion and the notable increase in voltage magnitude and stability. Moving forward, future research directions could focus on optimizing the design and control strategies of the LC filter to enhance its efficiency and adaptability under various operating conditions, as well as exploring its scalability and applicability in larger grid systems or microgrid configurations to further advance the transition towards cleaner and more sustainable energy systems.

## Acknowledgement

I would like to thank department of electrical engineering, Ahmadu Bello University Zaria, Nigeria, for providing us with high computing facilities and supervision on this work.

## REFERENCES


[1] A. M. Patel, "THD Comparison for 180, 120 & 150 Degree Conduction Mode of Three Phase Inverter," *International Journal for Scientific Research & Development*, vol. 6, no. 03, pp. 145–149, 2018, https://www.ijsrd.com/articles/IJSRDV6I30053.pdf.

[2] B. L. Dokić, B. Blanuša, "Introduction to Multilevel Converters," *Power* Electronics, 2014, https://doi.org/10.1007/978-3-319-09402-1_10.

[3] M. Bouchard, "Power Semiconductor Devices," *Springer*, 2020.

[4] O. O. Omitola, S. O. Olatinwo, T. R. Oyadore, "Design and Construction of 1KW (1000VA) Power Inverter," *Innovative Systems Design and Engineering*, vol. 5, no. 2, pp. 1-13, 2014, https://www.iiste.org/Journals/index.php/ISDE/article/view/11144.

[5] B. K. Bose, "Modern Power Electronics and AC Drives," *Prentice Hall PTR*, 2001, https://docs.google.com/file/d/0B_gTrLYkYZgzWTBvN0NSVlhDMms/edit?pref=2&pli=1&resourcekey=0-b0paf8MrHAPqavuz8Fs_sA.

[6] J. A. Ajiboye, C. Anene, M. A. Ajiboye, A. U. Usman, "Design and Implementation of a 5 kVA Inverter, *The IUP Journal of Electrical and Electronics Engineering (IJEEE),* vol. 9, no. 4, 2016, http://repository.futminna.edu.ng:8080/jspui/handle/123456789/15615.

[7] F. Asadi, N. Abut, "KUCA: Kocaeli University Converter Analysis simulation software in power electronics," *International Journal of Advanced and Applied Sciences*, vol. 3, no. 12, pp. 55-61, 2016, https://doi.org/10.21833/ijaas.2016.12.008.

[8] J. A. Momoh, *Energy processing and smart grid*, John Wiley & Sons, 2018, https://books.google.co.id/books?hl=en&lr=&id=ORxgDwAAQBAJ&oi=fnd&pg=PR1&dq=#v=onepage&q&f=false.

[9] M. Ciobotaru, R. Teodorescu and F. Blaabjerg, "Control of single-stage single-phase PV inverter," *2005 European Conference on Power Electronics and Applications*, p. 10, 2005, https://doi.org/10.1109/EPE.2005.219501.

[10] K. Ravi, Introduction to Different Types of Inverters, 2018.

[11] R. S. Singh, B. Pattanayak, S. Kumar, "Power Electronics: Computer Simulation and Analysis, *NIT Rourkela*, 2014, https://citeseerx.ist.psu.edu/document?repid=rep1&type=pdf&doi=61bbbce0de788d673d615f40623bf260dcfbcff0.

[12] M. Alsayed, M. Cacciato, G. Scarcella and G. Scelba, "Multicriteria Optimal Sizing of Photovoltaic-Wind Turbine Grid Connected Systems," in *IEEE Transactions on Energy Conversion*, vol. 28, no. 2, pp. 370-379, 2013, https://doi.org/10.1109/TEC.2013.2245669.

[13] T. Ma, H. Yang, L. Lu, J. Peng, "Technical feasibility study on a standalone hybrid solar-wind system with pumped hydro storage for a remote island in Hong Kong. Renew," *Renewable* Energy, vol. 69, pp. 7-15, 2014, https://doi.org/10.1016/j.renene.2014.03.028.

[14] M. Z. Youssef, K. Woronowicz, K. Aditya, N. A. Azeez and S. S. Williamson, "Design and Development of an Efficient Multilevel DC/AC Traction Inverter for Railway Transportation Electrification," in *IEEE Transactions on Power Electronics*, vol. 31, no. 4, pp. 3036-3042, 2016, https://doi.org/10.1109/TPEL.2015.2448353.

[15] M. Z. Youssef, M. Orabi and M. Tarbouchi, "Design of an efficient multilevel inverter for a 1500V railway propulsion system applications," *2015 IEEE Applied Power Electronics Conference and Exposition (APEC)*, pp. 1197-1201, 2015, https://doi.org/10.1109/APEC.2015.7104499.

[16] S. Ranjan and S. K. Mishra, "Analysis of asymmetrical cascaded multilevel inverter for traction systems," *2013 International Conference on Energy Efficient Technologies for Sustainability*, pp. 708-713, 2013, https://doi.org/10.1109/ICEETS.2013.6533472.

[17] M. Ali, M. M. Khan, Z. Yi, Y. J. Yang and H. Tang, "7-Level asymmetrical hybrid cascaded multilevel converter topology for traction system," *2017 International Conference on Electrical Engineering (ICEE)*, pp. 1-6, 2017, https://doi.org/10.1109/ICEE.2017.7893429.

[18] B. S. Revathi, M. Prabhakar, "Non-isolated high gain DC-DC converter topologies for PV applications-A comprehensive review," Renewable and Sustainable Energy Reviews, vol. 66, pp. 920-933, 2016, https://doi.org/10.1016/j.rser.2016.08.057.

[19] S. Peyghami, P. Palensky and F. Blaabjerg, "An Overview on the Reliability of Modern Power Electronic Based Power Systems," in *IEEE Open Journal of Power Electronics*, vol. 1, pp. 34-50, 2020, https://doi.org/10.1109/OJPEL.2020.2973926.

[20] B. Zhao, X. Zhang, P. Li, K. Wang, M. Xue, C. Wang, "Optimal sizing, operating strategy and operational experience of a stand-alone microgrid on Dongfushan Island," *Applied Energy*, vol. 113, pp. 1656-1666, 2014, https://doi.org/10.1016/j.apenergy.2013.09.015.

[21] V. Kuhn, J. Klemeš, I. Bulatov, "MicroCHP: Overview of selected technologies, products and field test results," *Applied Thermal Engineering*, vol. 28, 2039-2048, 2008, https://doi.org/10.1016/j.applthermaleng.2008.02.003.

[22] N. Patel, N. Gupta, B. C. Babu, "Design, Development, and Implementation of Grid-Connected Solar Photovoltaic Power Conversion System," *Energy Sources, Part A: Recovery, Utilization, and Environmental Effects*, vol. 43, pp. 2915-2934, 2019, https://doi.org/10.1080/15567036.2019.1668506.

[23] Y. Wang, C. K. Ahn, H. Yan and S. Xie, "Fuzzy Control and Filtering for Nonlinear Singularly Perturbed Markov Jump Systems," in *IEEE Transactions on Cybernetics*, vol. 51, no. 1, pp. 297-308, 2021, https://doi.org/10.1109/TCYB.2020.3004226.

[24] A. M. Noman, A. Alkuhayli, A. A. Al-Shamma'a, K. E. Addoweesh, "Hybrid MLI Topology Using Open-End Windings for Active Power Filter Applications," *Energies*, vol. 15, no. 17, p. 6434, 2022, https://doi.org/10.3390/en15176434.
[25] P. U. Panati, S. Ramasamy, M. Ahsan, J. Haider, E. M. G. Rodrigues, "Indirect Effective Controlled Split Source Inverter-Based Parallel Active Power Filter for Enhancing Power Quality," *Electronics*, vol. 10, no. 8, p. 892, 2021, https://doi.org/10.3390/electronics10080892.
[26] R. S. R. Chilipi, N. Al Sayari, K. H. Al Hosani and A. R. Beig, "Adaptive Notch Filter-Based Multipurpose Control Scheme for Grid-Interfaced Three-Phase Four-Wire DG Inverter," in *IEEE Transactions on Industry Applications*, vol. 53, no. 4, pp. 4015-4027, 2017, https://doi.org/10.1109/TIA.2017.2676098.
[27] M. Shahzad, K. V S Bharath., M. A. Khan and A. Haque, "Review on Reliability of Power Electronic Components in Photovoltaic Inverters," *2019 International Conference on Power Electronics, Control and Automation (ICPECA)*, pp. 1-6, 2019, https://doi.org/10.1109/ICPECA47973.2019.8975585.
[28] C. V. Pop, A. Buzo, G. Pelz, H. Cucu and C. Burileanu, "The Estimation of the Lifetime Variation for Power Devices," in *IEEE Transactions on Device and Materials Reliability*, vol. 19, no. 4, pp. 654-663, 2019, https://doi.org/10.1109/TDMR.2019.2940672.
[29] C. Bhargava *et al.*, "Review of Health Prognostics and Condition Monitoring of Electronic Components," in *IEEE Access*, vol. 8, pp. 75163-75183, 2020, https://doi.org/10.1109/ACCESS.2020.2989410.
[30] A. Hanif, Y. Yu, D. DeVoto and F. Khan, "A Comprehensive Review Toward the State-of-the-Art in Failure and Lifetime Predictions of Power Electronic Devices," in *IEEE Transactions on Power Electronics*, vol. 34, no. 5, pp. 4729-4746, 2019, https://doi.org/10.1109/TPEL.2018.2860587.
[31] H. Fathabadi, "Novel highly accurate universal maximum power point tracker for maximum power extraction from hybrid fuel cell/photovoltaic/wind power generation systems," *Energy*, vol. 116, pp. 402-416, 2016, https://doi.org/10.1016/j.energy.2016.09.095.
[32] H. Fathabadi, "Novel fast and high accuracy maximum power point tracking method for hybrid photovoltaic/fuel cell energy conversion systems," *Renewable Energy*, vol. 106, pp. 232-242, 2017, https://doi.org/10.1016/j.renene.2017.01.028.
[33] H. Fathabadi, "Novel high-efficient unified maximum power point tracking controller for hybrid fuel cell/wind systems," *Applied Energy*, vol. 183, pp. 1498-1510, 2016, https://doi.org/10.1016/j.apenergy.2016.09.114.
[34] "PSIM–Power Electronics Simulation Software," *Powersim Inc*, https://powersimtech.com/.
[35] PSIM SIMCAD, (2018).
[36] PSIM SIMCAD, PSIM user's guide, 2018.
[37] R. F. V. P. "Power electronics converters, applications and design," *Microelectronics Journal*, vol. 28, no. 1, pp. 105-106, 1997, https://www.elibrary.ru/item.asp?id=341857.
[38] R. Senthilkumar, M. Singaaravelu, "Design of Single Phase Inverter Using dsPIC30F4013," International Journal Engineering Research & Technology (IJERT), vol. 2, 6500-6506, 2012, https://www.ijert.org/.
[39] D. Solatialkaran, F. Zare, T. K. Saha and R. Sharma, "A Novel Approach in Filter Design for Grid-Connected Inverters Used in Renewable Energy Systems," in *IEEE Transactions on Sustainable Energy*, vol. 11, no. 1, pp. 154-164, 2020, https://doi.org/10.1109/TSTE.2018.2887079.
[40] F. A. Samman, M. Hasan and T. Damayanti, "Design and analysis of DC/AC inverter using passive LCL filter with damping circuit configuration," *2017 International Seminar on Intelligent Technology and Its Applications (ISITIA)*, pp. 46-51, 2017, https://doi.org/10.1109/ISITIA.2017.8124053.
[41] P. Mishra and R. Maheshwari, "Design, Analysis, and Impacts of Sinusoidal LC Filter on Pulsewidth Modulated Inverter Fed-Induction Motor Drive," in *IEEE Transactions on Industrial Electronics*, vol. 67, no. 4, pp. 2678-2688, 2020, https://doi.org/10.1109/TIE.2019.2913824.
[42] Z. Zou, Z. Wang and M. Cheng, "Modeling, Analysis, and Design of Multifunction Grid-Interfaced Inverters With Output LCL Filter," in *IEEE Transactions on Power Electronics*, vol. 29, no. 7, pp. 3830-3839, 2014, https://doi.org/10.1109/TPEL.2013.2280724.
[43] W. Wu, J. Ji and F. Blaabjerg, "Aalborg Inverter - A New Type of "Buck in Buck, Boost in Boost" Grid-Tied Inverter," in *IEEE Transactions on Power Electronics*, vol. 30, no. 9, pp. 4784-4793, 2015, https://doi.org/10.1109/TPEL.2014.2363566.
[44] B. Guo *et al.*, "Optimization Design and Control of Single-Stage Single-Phase PV Inverters for MPPT Improvement," in *IEEE Transactions on Power Electronics*, vol. 35, no. 12, pp. 13000-13016, 2020, https://doi.org/10.1109/TPEL.2020.2990923.
[45] G. S. Babu, U. K. Choudhury, G. TulasiramDas, and A. M. Kumar, "an Economical Approach of Designing a Three Phase Grid Tied Inverter for Solar Applications," *Int. J. Electr. Electron. Eng. Telecommun.*, vol. 1, no. 1, pp. 30–42, 2012, https://www.ijeetc.com/v1/ijeetc_v1_4_A008.pdf.
[46] Hardisal *et al.*, "Filter Component Impact on EGS002-based Inverter Circuit Performances," *IOP Conference Series: Materials Science and Engineering*, vol. 1062, no. 1, 2021, https://doi.org/10.1088/1757-899X/1062/1/012050.
[47] X. Wang, R. Zhuang, and J. Cai, "Theoretical Analysis of a Fractional-Order LLCL Filter for Grid-Tied Inverters," *Fractal and Fractional*, vol. 7, no. 2, p. 135, 2023, https://doi.org/10.3390/fractalfract7020135.
[48] S. S. Raghuwanshi, A. Singh, Y. Mokhariwale, "A comparison & performance of simulation tools MATLAB/SIMULINK, PSIM & PSPICE for power electronics circuits," *International Journal of Advanced*

*Research in Computer Science and Software Engineering*, vol. 2, no. 3, pp. 187-191, 2012, https://journals.indexcopernicus.com/search/details?id=40178.
[49] T. Rahman, S. M. A. Motakabber and M. I. Ibrahimy, "Design of a Switching Mode Three Phase Inverter," *2016 International Conference on Computer and Communication Engineering (ICCCE)*, pp. 155-160, 2016, https://doi.org/10.1109/ICCCE.2016.43.
[50] V. K. Arun Shankar, S. Umashankar, S. Paramasivam, Y. Venkatesh, K. Venkatesh and K. N. Dileep Sailesh, "Mathematical modelling and investigation of reduced order induction motor drive system," *2017 Innovations in Power and Advanced Computing Technologies (i-PACT)*, pp. 1-8, 2017, https://doi.org/10.1109/IPACT.2017.8244997.
[51] Y. Kim, H. Cha, B. -M. Song and K. Y. Lee, "Design and control of a grid-connected three-phase 3-level NPC inverter for Building Integrated Photovoltaic systems," *2012 IEEE PES Innovative Smart Grid Technologies (ISGT)*, pp. 1-7, 2012, https://doi.org/10.1109/ISGT.2012.6175663.
[52] H. Karami, M. Gandomkar, Z. Gandomkar, "Experimental Investigation of a Single-Phase Grid-Connected Inverter Equipped with an LC Filter for Photovoltaic Applications," *IEEE Transactions on Sustainable Energy*, vol. 9, no. 4, 2016, https://doi.org/10.1109/TSTE.2018.2793589.
[53] X. Nguyen, "Experimental Study on a Three-Phase Grid-Connected Inverter with LC Filter for Renewable Energy Applications," *Energies*, vol. 12, no. 18, p. 3541, 2019, https://doi.org/10.3390/en12183541.
[54] R. B., Manjes, "Analysis of THD and Harmonics in 3 Level Inverter with LC filter," *ITSI Transactions on Electrical and Electronics Engineering*, vol. 2, no. 2, pp. 30-34, 2014, http://www.irdindia.in/journal_itsi/pdf/vol2_iss4/7.pdf.